Title
SPIN-WAVE TURBULENCE

Authors
Bryant, P.
Jeffries, C.
Nakamura, K.

Publication Date
1987-02-01

Lawrence Berkeley Laboratory
UNIVERSITY OF CALIFORNIA

Materials & Chemical Sciences Division

Presented at the International Conference on The Physics of Chaos and Systems far from Equilibrium, Monterey, CA, January 11–14, 1987

SPIN-WAVE TURBULENCE

P. Bryant, C. Jeffries, and K. Nakamura

February 1987

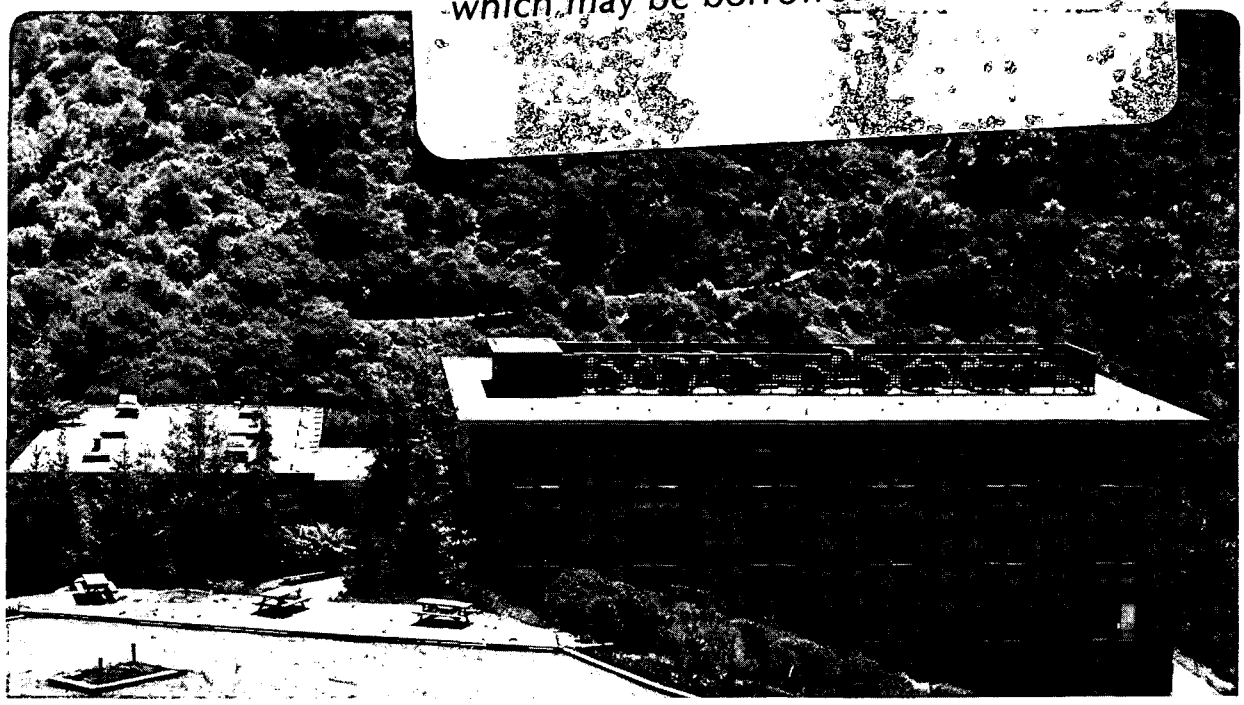

Prepared for the U.S. Department of Energy under Contract DE-AC03-76SF00098

DISCLAIMER

SPIN-WAVE TURBULENCE*

Paul Bryant and Carson Jeffries

Department of Physics and
Materials and Chemical Sciences Division,
Lawrence Berkeley Laboratory,
University of California, Berkeley, CA 94720

and

Katsuhiro Nakamura

Fukuoka Institute of Technology,
Higashi-ku, Fukuoka, 811-02, Japan

February 1987

*Supported in part by Director, Office of Energy Research, Office of Basic Energy Sciences, Materials Sciences Division of the U.S. Department of Energy under Contract No. DE-AC03-76SF00098.

Presented at the International Conference on
The Physics of Chaos and Systems Far from Equilibrium,
Monterey, CA, Jan. 11-14, 1987; Conference Proceedings
to be published in Nuclear Physics B (North-Holland Publishers).

LBL-23041

SPIN-WAVE TURBULENCE

Paul BRYANT,* Carson JEFFRIES,* and Katsuhiro NAKAMURA+

Physics Department, University of California, and Materials and Molecular Research Division, Lawrence Berkeley Laboratory, Berkeley, CA 94720, USA

A high resolution study is made of spin-wave dynamics above the Suhl threshold in a sphere of yttrium iron garnet driven by microwave ferromagnetic resonance. In different regions of parameter space observed behavior includes: excitation of a single spatial spin-wave mode at threshold; when two modes are excited, low frequency collective oscillations with a period doubling route to chaos; nonperiodic relaxation oscillations; when three modes are excited, quasiperiodic route to chaos; abrupt hysteretic onset of wide-band chaos. These results are accounted for in a unified way by numerical iteration of a model: coupled quantum oscillators representing the photons of the cavity and the magnons, including four-magnon scattering processes.

1. INTRODUCTION

Spin-wave instabilities were first observed by Damon[1] and Bloembergen and Wang[2]: microwave resonance in ferrites, when strongly driven, showed onset of anomalous absorption. Noisy low frequency oscillations were also discovered.[3] To fix ideas consider spin $\vec{S}_j$ on the crystal lattice of a ferrite sphere in an external magnetic field $\vec{H}_0$, with a hamiltonian

$$\mathcal{H} = -\hbar\gamma\Sigma_j \vec{S}_j\cdot\vec{H}_0 - 2J\Sigma_{j,j'} \vec{S}_j\cdot\vec{S}_{j'} + \Sigma H_{\text{dipole-dipole}} \qquad (1)$$

where γ is the gyromagnetic ratio and J (J>0) the Heisenberg nearest neighbor exchange energy. The Zeeman interaction leads to a uniform precession of the crystal magnetization M about H_0 at frequency $\omega_0 \equiv \gamma H_0$ and to a narrow ferromagnetic resonance absorption at $\omega_p \simeq \omega_0$ when driven by a small ac field $H_1 \sin(\omega_p t)$, perpendicular to H_0. The exchange term can give rise to spin-waves; the overall dispersion relation for Eq. (1) is[4]

$$\omega_k^2 = (\omega_0 - \frac{\omega_M}{3} + \gamma D k^2)(\omega_0 - \frac{\omega_M}{3} + \gamma D k^2 + \omega_M \sin^2\theta_k) \qquad (2)$$

for spin-waves of frequency ω_k and wave vector k in the direction θ_k relative to H_0. Here, M_s = sample magnetization, $\omega_M \equiv \gamma 4\pi M_s$, and the exchange constant

*Supported by Director, Office of Energy Research, Office of Basic Energy Sciences, Materials Sciences Division of the U.S. Department of Energy under Contract No. DE-AC03-76SF00098.

+Permanent address: Fukuoka Institute of Technology, Higashi-ku, Fukuoka, 811-02, Japan.

$D = 2JSa^2/\hbar\gamma$ Gcm^2. Nonlinear coupling between the uniform and spin-wave modes arises through the exchange and dipolar terms, which, for certain values of H_0 and pump frequency ω_p, gives rise to an instability: when the drive field H_1 is increased to a critical or "threshold" value H_{1c}, there is abrupt growth in the spin-wave excitation. A theory of this was given in 1957 by Suhl,[5] who remarked, "... this situation bears a certain resemblance to the turbulent state in fluid dynamics ...".

Suhl predicted several instabilities: (i) of first order when $\omega_p \approx 2\omega_k \sim 2\omega_0$ ("subsidiary absorption"); (ii) of second order when $\omega_p \approx \omega_k \approx \omega_0$ ("premature saturation"); (iii) and first order at $\omega_p \approx 2\omega_k$ with pump field H_1 parallel to H_0 ("parallel pumping"). An example of what can happen in case (i) is shown on the dispersion diagram, Fig. 1(a), computed from Eq. (2), with parameters valid for yttrium iron garnet (YIG) spheres ($\gamma = 17.7\times10^6$ G^{-1}sec^{-1}, $D = 5.4 \times 10^{-9}$ Gcm^2, $4\pi M_s = 1700$ G) and for pump frequency $\omega_p = 2\pi \times 9.2$ GHz, and for $\omega_0 = \gamma H_0 = 0.5\ \omega_p$, corresponding to $H_0 = 1640$ G; however, the exact condition $\omega_p = 2\omega_0$ is not required. Spin-waves can exist in the manifold shown, $0 \le \theta_k \le \pi/2$. How can they be excited? By a three-magnon scattering process[6]: a pump photon with $\omega_p \approx 2\omega_k$ can excite a uniform magnon $(\omega_p,k=0)_{mag}$ which scatters into a pair of magnons, (ω_k,k) and $(\omega_k,-k)$, i.e. a standing spin-wave mode, with locus along the dashed line, Fig. 1(a). Since the maximum wave vector, $k \approx 10^5$ cm^{-1}, is much larger than the fundamental wave vector $k_0 = \pi/d$ for a sphere of diameter $d \sim 10^{-1}$ cm, a large number of spin-wave modes are possible; they are damped at a rate $\gamma_k \sim 10^6$ sec^{-1}, typically, by magnon-phonon processes. Cases (ii) and (iii) are similar; in all cases microwave photons excite spin-waves of frequency $\sim10^{10}$ Hz.

Although these Suhl instabilities were extensively studied[7] earlier, no clear evidence of low dimensional chaotic motion was reported. Nakamura et al.[8] and Ohta and Nakamura[9] reexamined the theory for parallel pumping, numerically iterated the equations of motion assuming two modes, and found onset of instability, collective oscillations, and a period doubling cascade to chaos, with a Henón-like return map. Gibson and Jeffries[10] observed a period doubling route to chaos, periodic windows, and a single-hump return map for the second order instability in YIG. Zhang and Suhl[11] iterated the original equations for this instability and found a period doubling cascade to chaos. Similar theoretical conclusions were reported by Rezende et al.[12]; de Aguiar and Rezende[13] reported theory and experiments on parallel pumping.

In this paper we report a high resolution study of the first order instability in a YIG sphere. New findings indicate: a two-parameter (H_0,H_1^2) phase diagram; excitation of single modes; collective oscillations with quasiperiodicity, locking and chaos; and abrupt onset of high-dimensional

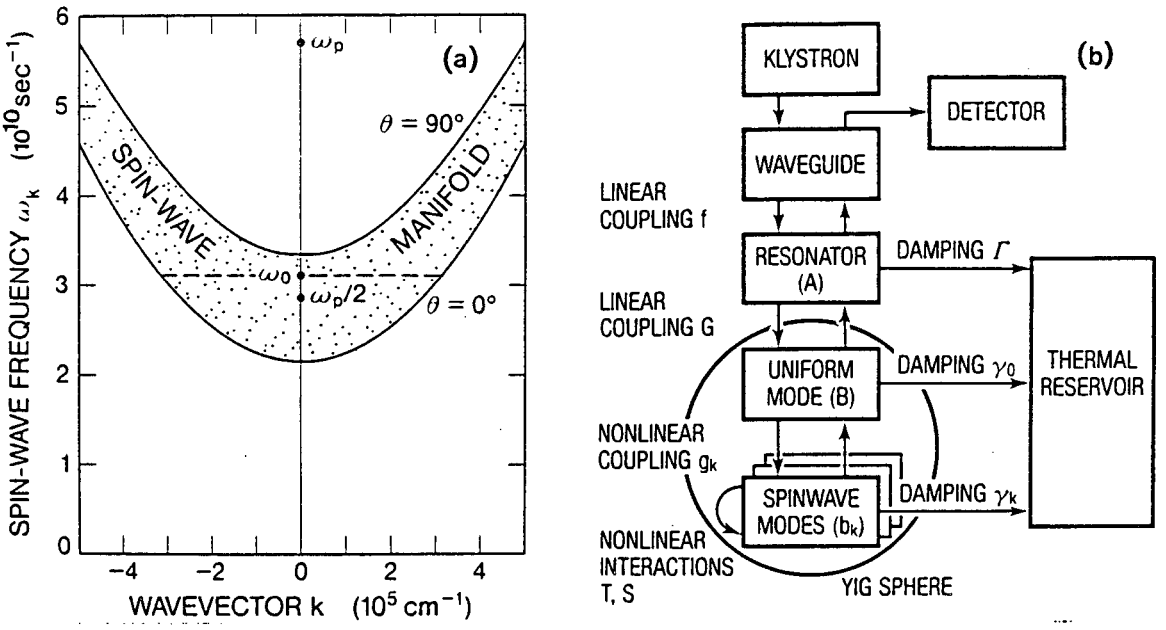

FIGURE 1
(a) Dispersion diagram, ω_k vs. k, from Eq. (2) for YIG sphere. (b) Diagram of experimental arrangement and model, Eq. (3).

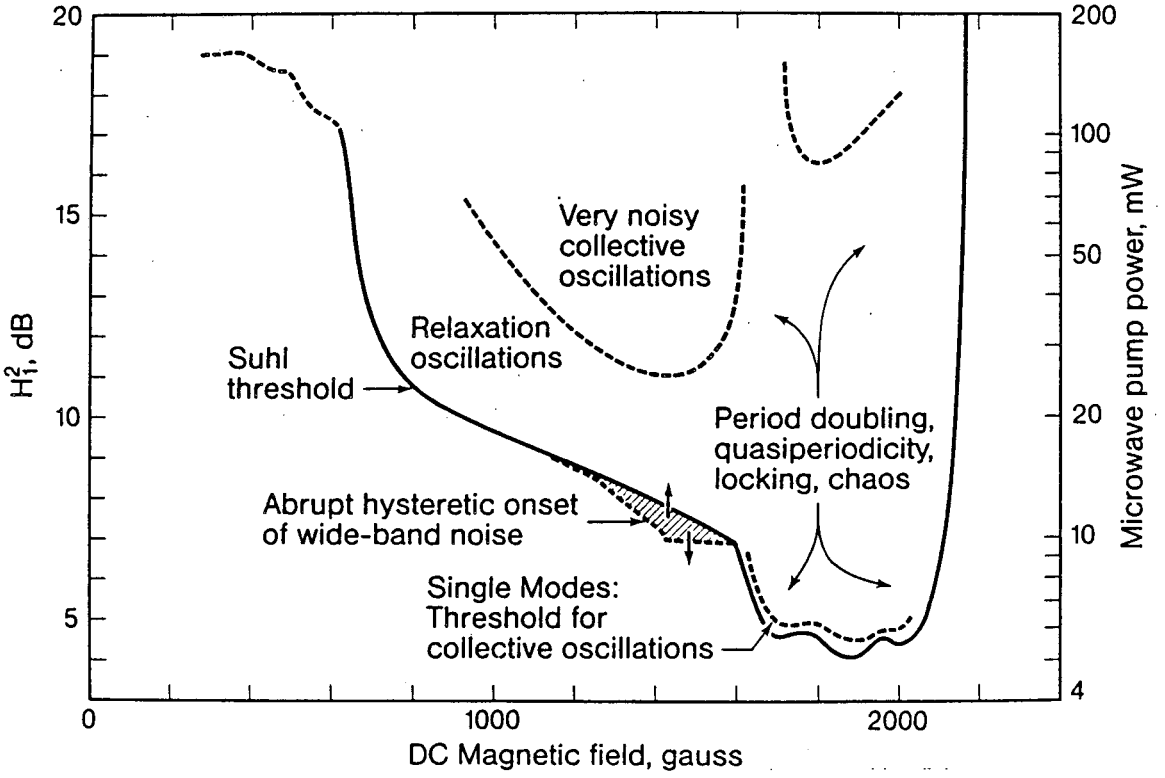

FIGURE 2
Regions and boundaries of observed behavior in parameter space (H_0,H_i^2).

turbulence with hysteresis. We present, in Sec. 3, a theoretical model to account for these in a unified way.

2. EXPERIMENTS

Figure 1(b) indicates schematically the experimental arrangement as well as the theoretical model. Microwave power from a klystron (f_p = 9.200 GHz) is coupled via a precision attenuator into a waveguide, and into a resonator, producing a field $H_1 \sin(2\pi f_p t)$ on the YIG sphere, oriented with the [111] axis parallel to a uniform and adjustable field H_0. The sphere of diameter 0.066 cm is spherical to within $\Delta R/R = 6 \times 10^{-5}$ and highly polished, to within 0.15 μm. Incident power P is absorbed by the resonator (A), and the uniform mode (B), and the spin-wave modes (b_k). Power not absorbed is reflected onto a diode detector giving a dc signal S_0 as well as an ac signal S(t) (100 Hz to 1 MHz). This paper mainly reports on the subsidiary absorption instability ($H_1 \perp H_0$), although some data are given for parallel pumping ($H_1 \parallel H_0$), to be reported separately.[14]

Figure 2 shows regions and boundaries of observed behavior in the space of two parameters: dc field H_0 and microwave pump power $P \propto H_1^2$. The Suhl threshold boundary is found by monitoring signal S_0, which drops at onset of any spin-wave excitation. This boundary is abrupt and reversible except near the shaded area, where onset is abrupt and hysteretic, and accompanied by a large signal S(t) of wideband character (~ MHz) with no resolvable spectral peaks. For $H \lesssim 600$ G the boundary becomes increasingly less distinct.

For $H_0 \gtrsim 1600$ G and P ~ 0.1 dB above the Suhl threshold we generally find onset of sinusoidal "auto" oscillations [Fig. 3(a)] in the frequency range $10^4 \lesssim f_{co} \lesssim 10^6$ Hz, which are believed to arise from coupling between spin-waves; we refer to them as "collective" oscillations. These oscillations show period doubling [Figs. 3(b), 4(a)] and a transition to chaos [Figs. 3(e), 4(b)]. The frequency has a marked dependence on pump power, Fig. 5(a), which is consistent with predictions, Fig. 5(b), of our model in Sec. 3, as well as that of Zautkin et al.[15] Typically these single frequency oscillations display a bifurcation to quasiperiodicity [Figs. 3(c), 3(d), 4(c)], along with frequency locking and chaos; they may appear when at least three spin-wave modes are excited. The spectral lines of these periodic oscillations are ~ 50 dB above a broad spectral base believed to be of deterministic origin. In some regions (H_0 ~ 1400 G, P ~ 50 mW) the base has a much higher intensity (+30 dB); the rough boundary for these noisy oscillations is shown in Fig. 2.

The parallel pumped instability is also observed, showing period doubling [Fig. 4(d)] to at least period eight, onset of quasiperiodicity, and chaos, Fig. 4(e). Another type of signal, nonperiodic "relaxation oscillation," Fig.

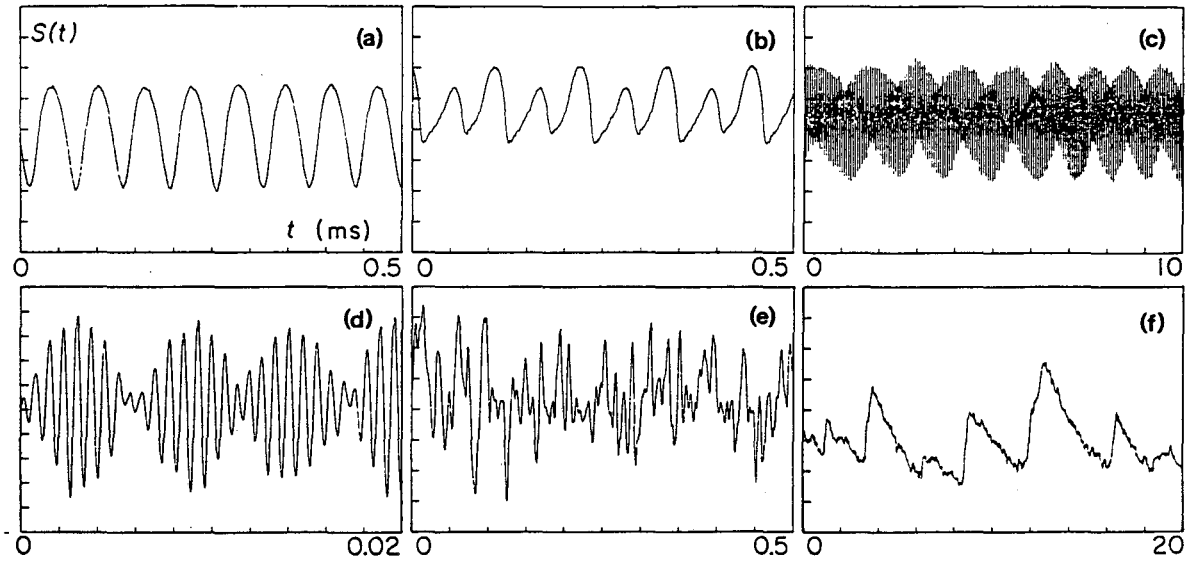

FIGURE 3
Observed signals, S(t) (relative units) vs. t, showing (a) periodic oscillations, $f_{CO} \approx 16$ kHz; (b) period doubled; (c) quasiperiodic; (d) quasiperiodic; (e) chaotic; (f) relaxation oscillation.

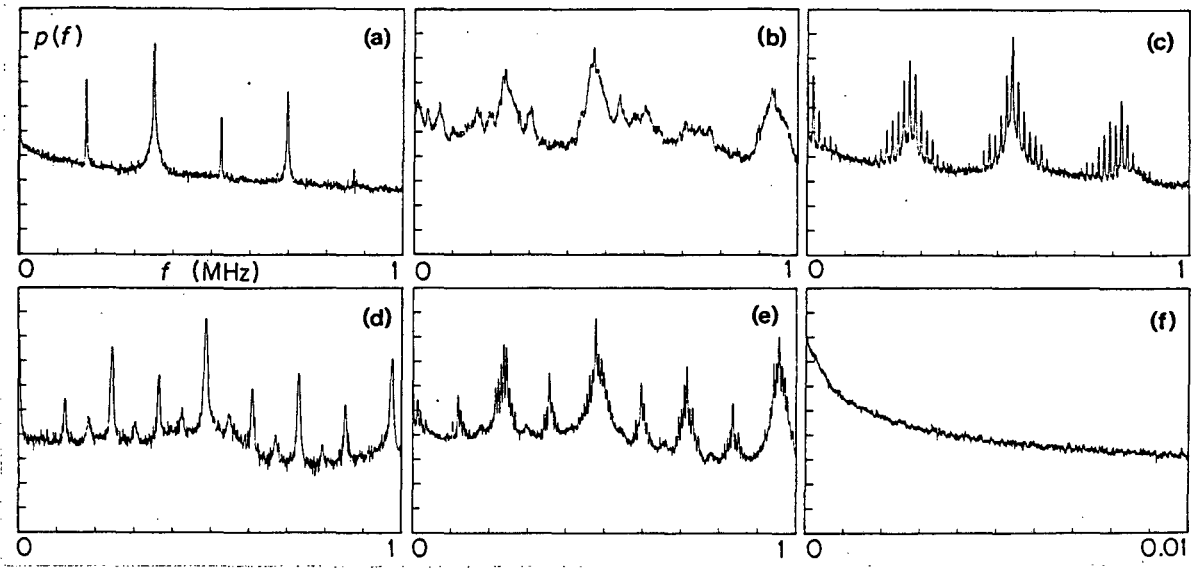

FIGURE 4
Observed power spectra, p(f) (10 dB/div) vs. f for: (a) period doubling; (b) onset of chaos; (c) quasiperiodicity; (d) parallel pumping, period doubling to period 8; (e) quasiperiodicity; (f) relaxation oscillations, Fig. 3(f).

3(f), is found in a broad region, Fig. 2; they have essentially no resolved spectral peaks, Fig. 4(f), and may be related to the "chaotic bursts" of the model below.

The Suhl threshld in the region $1600 \lesssim H_0 \lesssim 1900$ G, when examined at high resolution, has a rich structure, Fig. 5(c). For constant pump power, the dc signal S_0 vs. H_0 is recorded while slowly increasing H_0, showing a series of peaks in the power absorption spaced by $\Delta H_0 = 0.157$ G, which can be understood as high order spatial resonances of single spin-wave modes within the sphere.[16] In a simplified picture assume that the spin-wave mode $(\omega_k, \pm k)$ has an integral number n of half wavelengths that resonantly fit in the diameter d of the sphere if $n(\pi/d) = k$; if k is changed by $\Delta k_0 = \pi/d$, the next spatial resonance at n+1 will be excited. From Eq. (2) this small change Δk_0 can be induced by a field change ΔH_0 while holding constant $\omega_k = \omega_p/2$, if $\Delta H_0 = 2Dk\Delta k_0$. If we take $k \approx 3 \times 10^5$ cm^{-1} and $\theta = 0$ [Fig. 1(a)], this expression yields $\Delta H_0 = 0.152$ G in agreement with the observed splitting. Another sequence of modes will have a similar set of dips of slightly different spacing with the irregular interferences most clearly seen to the right in Fig. 5(c). In a more refined picture the dips in Fig. 5(c) may be viewed as the modes of a sphere M_{jkl}, say, labelled by suitable indices. We find that for the first few dips in S_0 only single modes are excited and are not accompanied by a collective oscillation signal S(t). Beyond this point simultaneous excitation of two or more modes becomes possible owing to mode overlap. Signals at $f_{co} \approx 10^5$ Hz may appear when a second mode becomes simultaneously excited; a second frequency f'_{co} may appear when a third mode is simultaneously excited.

3. THEORY

We model the system, Fig. 1(b), as a collection of coupled quantum oscillations, with the hamiltonain[7,8]

$$\begin{aligned}\mathcal{H} &= \hbar\omega_r A^+A + \hbar\omega_0 B^+B + \sum_k \hbar\omega_k b_k^+ b_k \\ &+ \hbar(G^* A^+ B + \text{h.c.}) + \frac{\hbar}{2}\sum_k (g_k^* B b_k^+ b_{-k}^+ + \text{h.c.}) \\ &+ \hbar\sum_{k,k'}(T_{kk} b_k^+ b_k b_{k'}^+ b_{k'} + \frac{1}{2} S_{kk'} b_k b_{-k} b_{k'}^+ b_{-k'}^+) + \hbar(FA^+\exp(-i\omega_p t) + \text{h.c.})\end{aligned} \tag{3}$$

These terms are, respectively: (1) a single oscillator with raising and lowering operators A^+, A representing a single electromagnetic mode of the resonator of frequency ω_r; (2) a single oscillator representing the uniform mode of frequency $\omega_0 = \gamma H_0$; (3) a set of oscillators representing spin-waves of frequency ω_k, Eq. (2), for all possible wave vectors k; (4) linear coupling G between resonator and uniform mode; (5) nonlinear coupling between uniform and spin

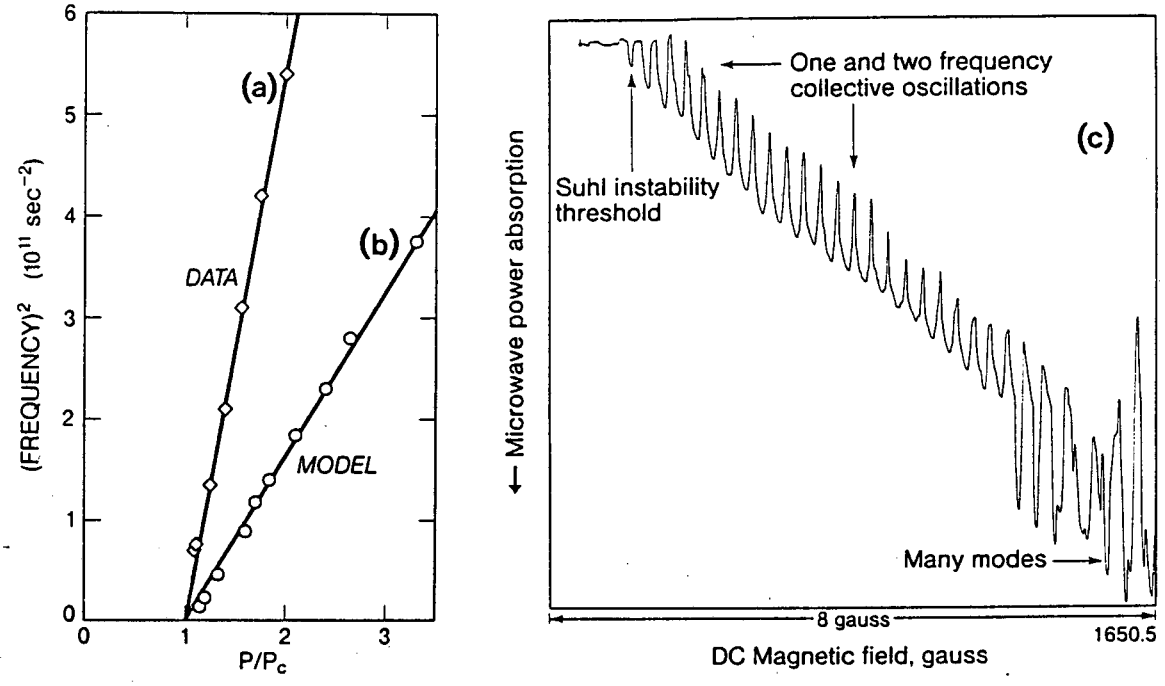

FIGURE 5

(a) Square of observed collective oscillation frequency f_{co}^2 vs. pump power P relative to threshold value P_c. The line is a fit to the data. (b) $10\times f_{co}^2$ vs. P/P_c, computed for two-mode model: the line has the same functional form as that of (a), $f_{co}^2 \propto \left((P/P_c)-1\right)$. (c) Observed single mode resonances.

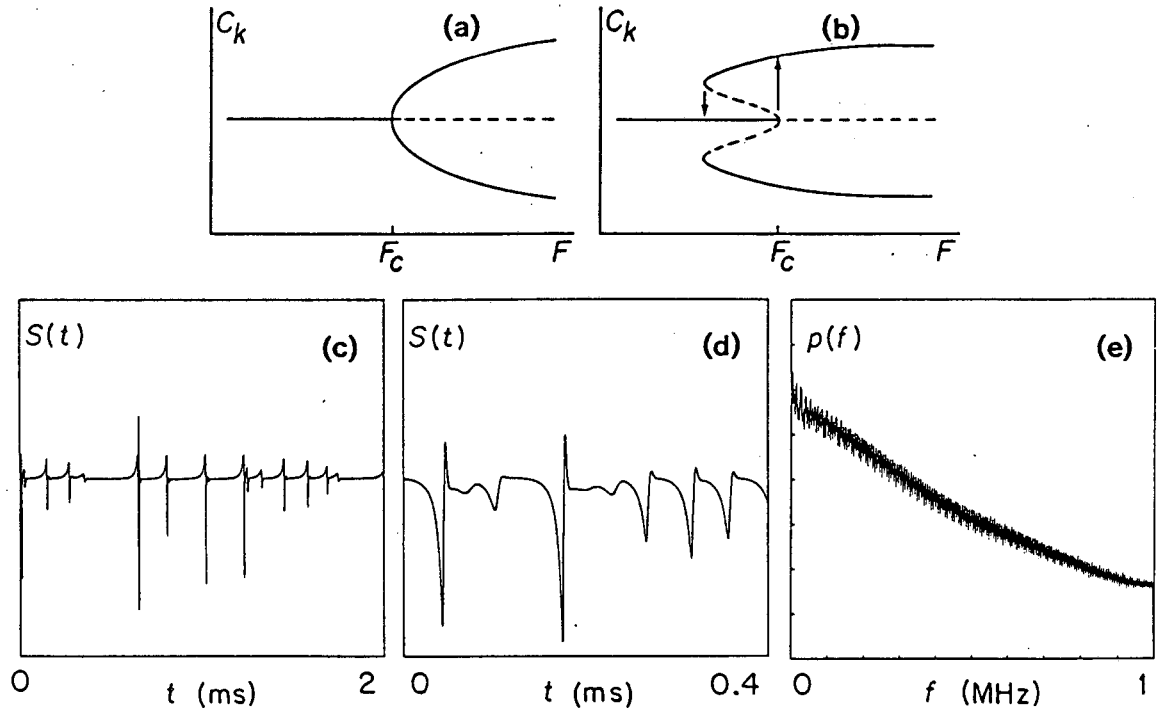

FIGURE 6

(a) Subcritical, and (b) supercritical symmetry-breaking bifurcations; center line is trivial fixed point $C_k=0$; dotted line represents unstable fixed points. (c) and (d) Time series of computed solution for two-mode model, showing "spiking" and "relaxation oscillations;" compare to Fig. 3(f). (e) Power spectrum of (d); compare to Fig. 4(f).

wave modes; (6) nonlinear wave-wave coupling from the four magnon interaction; (7) microwave driving of the resonator by the klystron of frequency ω_p and amplitude F. The pump power $P \propto F^2$. From Eq. (3) we obtain the equations of motion for A, B, and b_k, and then add phenomenological damping terms Γ, γ_o, γ_k, respectively.

Since $\omega_p \approx 10^{11}$ sec^{-1} and we are interested in signal frequencies ~0 to 10^7 sec^{-1}, we transform to slow variables $\tilde{A}$, $\tilde{B}$, and C_k using

$$\tilde{A} = A \exp(-i\omega_p t); \; \tilde{B} = B \exp(-i\omega_p t); \; b_k = C_k \exp(-\omega_p t/2) \tag{4}$$

Since waves are created in (k,-k) pairs we take $C_k = C_{-k}$, and $|C_k|^2$ becomes the magnon occupation number. This transformation introduces the "detuning" parameters

$$\Delta\Omega_o = \omega_o - \omega_p \sim 3 \times 10^{10} \text{ sec}^{-1} \tag{5a}$$

$$\Delta\Omega_k = (\omega_k - \omega_p/2) = 2\pi\nu_k \lesssim 10^6 \text{ sec}^{-1} \tag{5b}$$

$$\Delta\Omega_r = \omega_r - \omega_p, \text{ set to zero .} \tag{5c}$$

We make the approximation that the resonator has the greatest damping and thereby $\tilde{A}$ adiabatically follows $\tilde{B}$ and C_k. Since $\tilde{B}$ may oscillate rapidly due to large values of $\Delta\Omega_o$, we replace it by its average and regard the average of $\dot{\tilde{B}}$ as small. The only remaining dynamical variables are the C_k with equation

$$\dot{C}_k = -\gamma_k C_k - i\Delta\Omega_k C_k - iQFg_k^* C_k^* - i\sum_{k'}\{2T_{kk'}|C_{k'}|^2 C_k + (S_{kk'} + Eg_{k'}g_k^*)C_{k'}^2 C_{k'}^*\} \tag{6}$$

where k = 1,2,...N is an index for a spin-wave mode, k' = 1,2,...N, and parameters Q and E are functions of the parameters previously introduced. Equation (6) has the form of a set of N coupled damped driven nonlinear oscillators, each representing one spin-wave mode; there is always one uniform mode, somewhat hidden in these equations: $\tilde{B}$ depends on C_k as $\tilde{B} = QF + E\sum_{k'} g_{k'}C_{k'}^2$. We do not convert the variables C_k into Cooper-pair variables[7] since this obscures important symmetry properties of the system. For suitable parameter values[17] we numerically iterate Eq. (6), first for N = 1, then N = 2, etc., adding one mode at a time. Control parameters used include pump power P, and the detuning frequency ν_k [Eq. (5b)] corresponding to a change in the field H_o.

In Eq. (6) we note that $C_k = 0$ is always a solution or fixed point of the system. For small forcing F this is a stable fixed point, but it becomes unstable at the Suhl threshold where the forcing is first able to overcome the damping. Nonzero (or nontrivial) fixed points may also exist and have important consequences for the system's behavior. If we assume one mode to be excited, then we may determine these nontrivial fixed points exactly. The

equation $\dot{C}_k = 0$ can be put in the form:

$$M + N|C_k|^2 = \frac{(C_k^*)^2}{|C_k|^2} = \text{point on unit circle} \tag{7a}$$

where $$M = i(\gamma_k + i\Delta\Omega_k)/QFg_k^* \tag{7b}$$

and $$N = -(2T_{kk} + S_{kk} + E|g_k|^2)/QFg_k^* \tag{7c}$$

The Suhl threshold corresponds to $|M| = 1$, and the solution $C_k = 0$ is stable for $|M| > 1$ (note that M varies inversely with the forcing F). There are two distinct possibilities for what may occur when the threshold is crossed. For $\mathrm{Re}(M/N) \geq 0$ one obtains an ordinary (or supercritical) symmetry breaking bifurcation at the Suhl threshold. As the solution $C_k = 0$ becomes unstable, a complementary pair of stable nontrivial fixed points emerge from the origin, Fig. 6(a). (These two solutions are actually equivalent: one represents a shift in phase by π of the other.) The second possibility is that $\mathrm{Re}(M/N) < 0$ and a subcritical symmetry breaking bifurcation will occur. In this case, nontrivial fixed points first appear below the Suhl threshold via saddle-node bifurcation. As F crosses the Suhl threshold F_c, C_k jumps to one of these at a finite value, and the system will display hysteresis on reducing F, Fig. 6(b). In our experiments we observe a region of hysteresis, Fig. 2, which we believe is due to this effect.

Numerical iteration of Eq. (6) yields a wide variety of behavior, here summarized. With only one spin-wave mode allowed (in addition to the hidden uniform mode) a Suhl threshold is found, but no oscillations. For N = 2 modes an example of behavior follows: choosing parameters [Eq. (5b)] $\nu_1 = -60$ kHz, $\nu_2 = 40$ kHz, yields Suhl thresholds at pump power $P_1 = 8.43$ mW, $P_2 = 4.77$ mW, respectively, for C_1 and C_2. At P = 10 mW, C_2 has developed an asymmetric orbit at $f_2 = 97$ kHz, Fig. 7(a); and C_1 a symmetric orbit at $f_1 = (1/2)f_2$. Holding P = 10 mW but decreasing H_0 yields various computed behavior: for $\nu_1 = -77$ kHz, $\nu_2 = 23$ kHz we find period doubling for C_2, Fig. 7(c), and symmetry breaking for C_1, Fig. 7(d). For $\nu_1 = -82$ kHz, $\nu_2 = 18$ kHz, both orbits have become chaotic: Figs. 7(e) and (f) show this for mode C_2. At other parameter values, particularly when one mode is below and the other above Suhl threshold, nonperiodic "relaxation oscillations" are found, Fig. 6(c,d,e), rather similar to those observed experimentally [Figs. 2, 3(f), and 4(f)].

For N = 3 modes the computed behavior shows periodic orbits, then quasi-periodic as in the portrait of Fig. 8(a) and power spectrum, Fig. 8(b). A chaotic section is shown in Fig. 8(c), with power spectrum, Fig. 8(d); the orbits are apparently near, but not locked, to a 1:5 winding number. Unusual behavior is shown in the portrait and time series, respectively, in Fig.

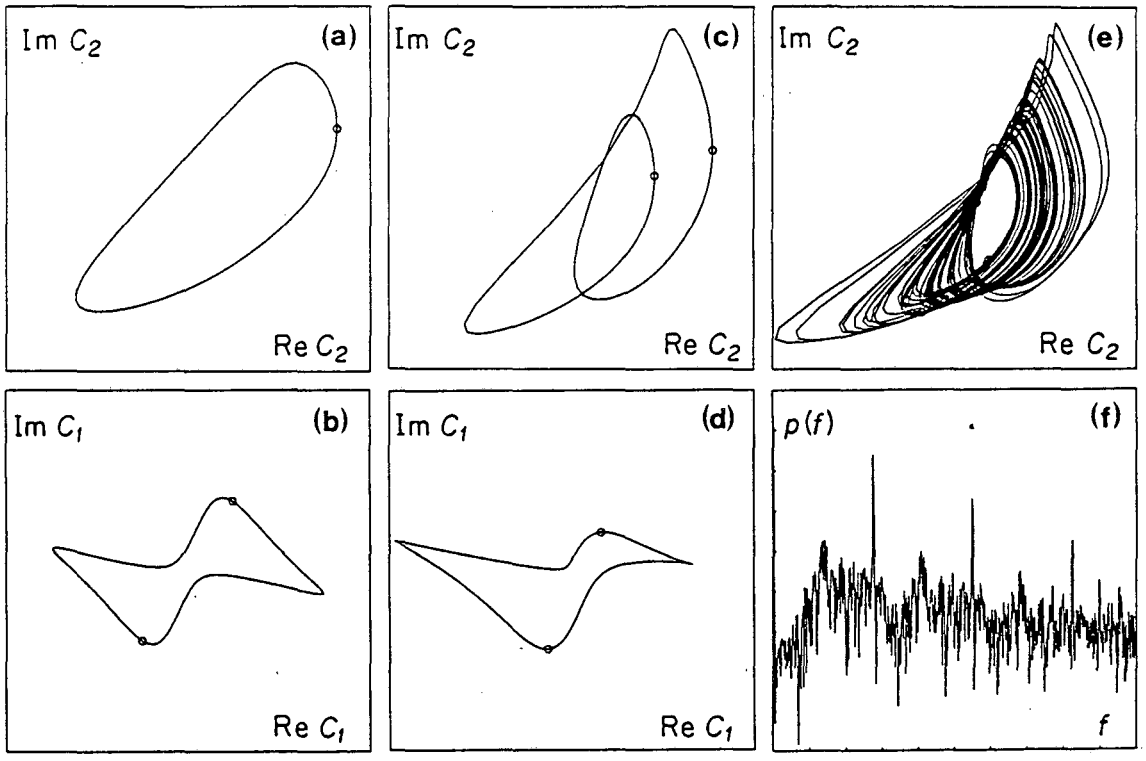

FIGURE 7
Computed behavior for two modes: (a) phase portrait for periodic oscillations, asymmetric mode; (b) symmetric mode; (c) period doubling; (d) symmetry breaking; (e) chaos; (f) power spectrum of above, f_{max} = 0.5 MHz.

8(e,f). This orbit appears to be of the Silnikov type, and may be related to that of Fig. 6(c) and (d), for N = 2 modes, but with additional high frequency components. Behavior qualitatively like this is observed in the experiment.

4. SUMMARY AND CONCLUSIONS

Starting from the viewpoint of microscopic scattering processes of spin waves on a magnetic crystal lattice, we make a connection to the theoretical framework of nonlinear dynamics. We specifically aim to elucidate the dynamical behavior of the magnetization in a finite sphere of a real material, yttrium iron garnet, above the Suhl first order instability, excited by microwave pumping. The model used is a collection of quantum oscillators representing the photons and magnons; effects of the cavity mode are included; the consequences of symmetry are investigated. In a high resolution (10^{-5}) experimental exploration of parameter space we find, on a global phase diagram, the regions and boundaries of a wide variety of behavior: (1) The Suhl threshold is found when, in addition to the uniform precession, a single

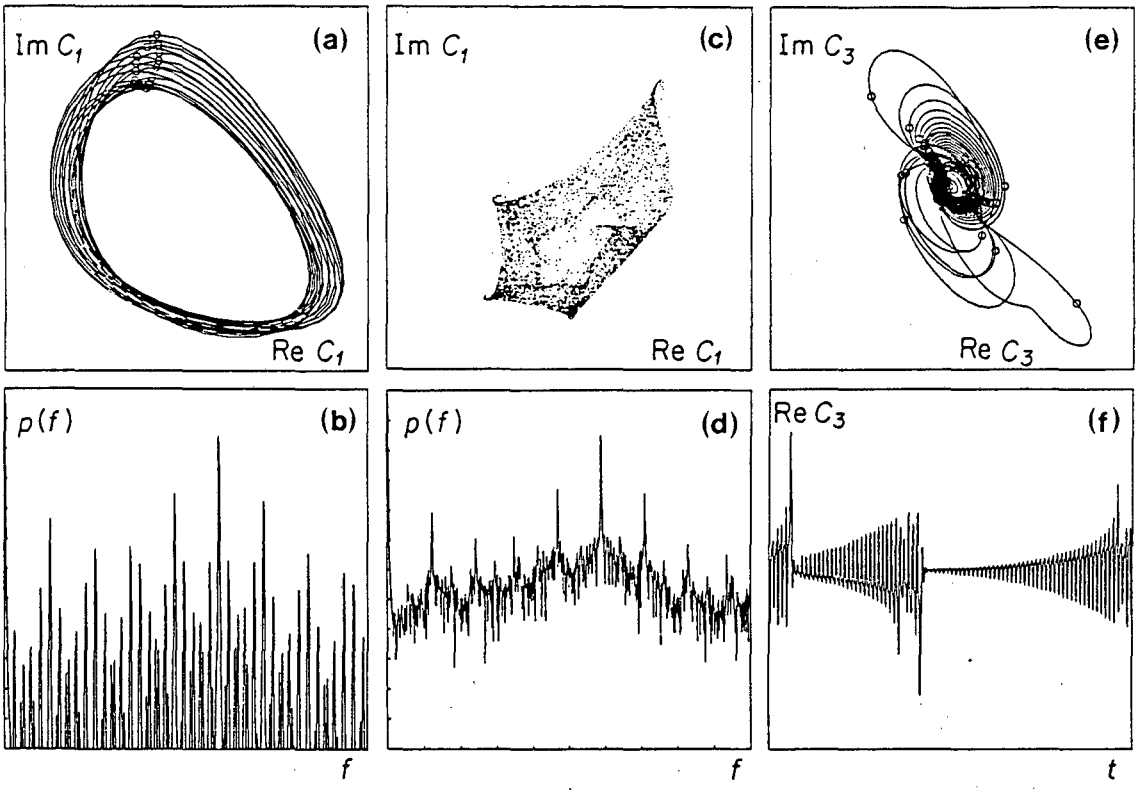

FIGURE 8
Computed behavior for three modes: (a) phase portrait of quasiperiodic orbit and section; (b) power spectrum of above; f_{max} = 0.25 MHz; (c) Poincaré section of orbit beyond quasiperiodic transition to chaos; (d) power spectrum of above; f_{max} = 0.25 MHz; (e) portrait of Silnikov-type orbit; (f) time series of above.

spatial spin-wave mode is excited, $f_1 \sim 10^{10}$ Hz. (2) When a second mode is excited, at $f_2 \sim 10^{10}$ Hz, there may occur onset of a low frequency collective oscillation, $f_{co} \sim 10^4$-10^6 Hz, owing to the coupling between the two microwave modes; the observed dependence of f_{co} on pump power is in agreement with the model. The oscillation f_{co} displays a period doubling route to chaos. (3) When a third mode is excited, an additional oscillation f'_{co} may arise, and the system then displays a quasiperiodiic route, including frequency locking and chaos. Regions (2) and (3) are closely intertwined. (4) There exists a small region characterized by abrupt hysteretic onset of wide-band chaos. (5) There is an extended region characterized by nonperiodic "relaxation" oscillations.

The model predicts the observed behavior in regions (1), (2), and (3), and also predicts behavior qualitatively like (4) and (5). For four modes excited, neither the experiment nor the model have yet yielded three-frequency quasi-periodicity; we expect this only in a very small region of parameter space. Further details will be published elsewhere.[14]

REFERENCES

1. R.W. Damon, Rev. Mod. Phys. 25 (1953) 239.

2. N. Bloembergen and S. Wang, Phys. Rev. 93 (1954) 72.

3. T.S. Hartwick, E.R. Peressini, and M.T. Weiss, J. Appl. Phys. 32 (1961) 2235.

4. A.M. Clogston, H. Suhl, L.R. Walker, and D.W. Anderson, J. Phys. Chem. Solids 1 (1957) 129.

5. H. Suhl, J. Phys. Chem. Solids 1 (1957) 209.

6. See, e.g., F. Keffer, Spin Waves, in Encyclo. of Physics 18/2, chief editor S. Flügge (Springer-Verlag, 1966).

7. For a review see V.E. Zakharov, V.S. L'vov, and S. S. Starobinets, Sov. Phys. Usp. 17 (1975) 896.

8. K. Nakamura, S. Ohta, and K. Kawasaki, J. Phys. C 15 (1982) L143.

9. S. Ohta and K. Nakamura, J. Phys. C 16 (1983) L605.

10. G. Gibson and C. Jeffries, Phys. Rev. A 29 (1984) 811.

11. X.Y. Zhang and H. Suhl, Phys. Rev. A 32 (1985) 2530.

12. S.M. Rezende, O.F. de Alcontara Bonfin, and F.M. de Aguiar, Phys. Rev. B 33 (1986) 5153.

13. F.M. de Aguiar and S.M. Rezende, Phys. Rev. Lett. 50 (1986) 1070.

14. P. Bryant, K. Nakamura, and C. Jeffries, to be published.

15. V.V. Zautkin, V.S. L'vov, and S.S. Starobinets, Sov. Phys. JETP 36 (1973) 96.

16. W. Jantz and J. Schneider, Phys. Stat. Solidi (a) 31 (1975) 595.

17. Typical values used for parameters: $G = 1.2 \times 10^{11}$ sec^{-1}, $g_k = 14$ sec^{-1}, $\Gamma = 10^8$ sec^{-1}, $\gamma_0 = 10^7$ sec^{-1}, $k = 2 \times 10^5$ sec^{-1}, $F = 4 \times 10^{14}$ sec^{-1}, $T_{kk} = -2 \times 10^{-8}$ sec^{-1}, $T_{kk'} = 0$, $S_{kk} = 4 \times 10^{-8}$ sec^{-1}, $S_{kk'} = 4.5 \times 10^{-8}$ sec^{-1}, $Q = (-8.5 \times 10^{-11} - i2 \times 10^{-12})$ sec, $E = (1.6 \times 10^{-14} - i7.3 \times 10^{-13})$ sec. These values are preliminary, and only approximately correspond to the real physical system.

This report was done with support from the Department of Energy. Any conclusions or opinions expressed in this report represent solely those of the author(s) and not necessarily those of The Regents of the University of California, the Lawrence Berkeley Laboratory or the Department of Energy.

Reference to a company or product name does not imply approval or recommendation of the product by the University of California or the U.S. Department of Energy to the exclusion of others that may be suitable.

LAWRENCE BERKELEY LABORATORY
TECHNICAL INFORMATION DEPARTMENT
UNIVERSITY OF CALIFORNIA
BERKELEY, CALIFORNIA 94720